Journal of Materials and Engineering Structures

Research Paper

Crashworthiness of Highway Lamp Post against Vehicle Impact

K. Senthil *, S. Rupali

Department of Civil Engineering, NIT Jalandhar, Jalandhar, Punjab 144011, India

ARTICLE INFO

Article history :

Received : 24 March 2018

Revised : 28 July 2018

Accepted : 15 August 2018

Keywords:

Steel Pole

Vehicle Impact

Finite Element Analysis

Failures and Damage

ABSTRACT

Three dimensional numerical investigations has been carried out on steel lamp post against vehicle impact using ABAQUS/Explicit finite element code. The response of steel pole was studied against vehicle impact subjected to varying speed and mass of vehicle, and varying thickness and impact location of pole. The geometry of steel pole was considered on the basis of Indian standard recommendations and choice of pole is based on conventional highway lighting applications supporting luminaire mounting heights. The constitutive and fracture behavior of steel pole has been predicted using JC model available in ABAQUS/Explicit and the material parameters of JC model for the available in literature. The response of metallic pole was studied against varying speed, mass of vehicle and impact location considering the influential factors which affects the pole significantly. In addition to that, the response of pole was studied against the varying thickness, i.e. the effective thickness of cylindrical pole may be decreased at later stage due to corrosion and environmental effects. The responses of steel pole have been studied and presented in light of reaction forces, deflection and Von-Mises stresses.

1 Introduction

The mitigation of severe problems due to vehicle collisions with roadside hardware has become one of the major research areas in the field of civil and automotive engineering. The hardware of roadside system includes barriers, light poles, closed-circuit television camera tower, overhead power transmission lines and security towers. Poles are generally called as posts which are made by either steel or concrete used widely as highway and street lighting systems as well as other structural applications. Nowadays, steel poles/systems are the most important part of the transportation system and whereas the systems are more vulnerable against heavy impact load and large deformations. A few researchers have investigated on both steel as well as concrete poles from various part of the world and a few studies are discussed here. Elmarakbi et al. [1] developed a finite element model using LS Dyna to simulate vehicle collision on traffic light pole examining five different poles as well as different soil types in which they were embedded. Detailed numerical analyses concluded that poles directly embedded in soil proves to be strong, flexible and offers least impact on vehicles as well as occupants. Le et al. [2] studied the natural frequencies of the long tapered hollow steel poles numerically using three-dimensional finite element analyses and verified

* *Corresponding author. Tel.: +91-9458948743/+91-8267927382.*
E-mail address: urssenthil85@yahoo.co.in; kasilingams@nitj.ac.in

e-ISSN: 2170-127X,

RESEARCH REVIEW of Sciences and Technologies

them with experimental data and also performed sensitivity analyses to determine the frequencies of poles. Jung et al. [3] conducted experimental and finite element investigations of the load-deformation behavior of tapered steel and fiber-reinforced plastic bridge camera poles subjected to cantilever bending type loading. The load-deformation obtained from finite-element analyses are compared with those of the experiments and found in good agreement. The behavior of the finite-element models is examined by observing the effects of individual geometric variables on the load-deformation characteristics of the poles.

Vivek et al. [4] studied the failure mechanism of lightly-embedded prestressed concrete poles against wind storms through field tests and verified with finite element results. It is observed that the load capacities of the poles have been found to be in the range of 0.95 to 1.48 times the design wind load. It was concluded that by increasing the footing dimension by 20%, the capacity of the pole is improved about 54%. Lu et al. [5] developed LPV-ARMAX model to simulate the car-to-pole collision with different initial impact velocities. The comparison between the predicted and the experimental test data is conducted, which shows the high fidelity of the LPV-ARMAX model. Sharma et al. [6] developed a method for estimating dynamic shear force capacity and demand of an RC column subjected to vehicle impact for different performance levels. It is concluded that the proposed method may be used for the design of RC columns to minimize damage and meet a set of performance objectives during different vehicle impact scenarios. Chen et al. [7] studied the dynamic response of concrete pole in car-pole collision by FE model. It is observed that the maximum longitudinal intrusion of the vehicle increased 13.9% as the speed increases from 30 to 70 km/h, while the proportion of energy absorbed by car to the kinetic energy decreased from 43.6% down to 14.6%. In addition, few more researchers have been working on the structural performance of the poles under dynamic loads in the past few years [8-10].

A detailed literature survey shows that few attempts in finite-element computer simulation of vehicle collision with roadside hardware have been conducted. It is observed that no effective numerical studies have been carried out in the field of behavior of pole subjected to vehicle impact, as well as it is expensive to practically conduct the experiments and practically not possible to produce the actual situations of the impact in practical experiments. However, limited research has been conducted to enhance the safety performance of traffic light poles when impacted by vehicles. In light of research gaps observed from the detailed literature survey, the objective of this paper is to study the behavior of steel lamp post subjected to vehicle impact through finite element simulations. The material parameters of the Johnson-Cook elasto-viscoplastic model were employed for predicting the behavior of the metallic poles is discussed in Section 2. A detailed numerical modelling of finite element simulations and mesh convergence study have been discussed in Section 3. The response of metallic pole was studied against varying speed and mass of vehicle considering the influential factors which affects the pole significantly. Also the response of pole was studied against the varying thickness, i.e. the effective thickness of cylindrical pole may be decreased at later stage due to corrosion and environmental effect. In addition to that, the pole was studied against the varying impact location and the location was varied from the base. The response of steel pole was studied in terms of stresses, deformation, and reaction forces by the steel pole and compared in Section 4.

2 Constitutive Modelling

The constitutive and fracture behavior of steel pole was predicted employing the Johnson-Cook [11] elasto-viscoplastic material model available in ABAQUS finite element program is discussed in this Section. The material model is based on the von Mises yield criterion and associated flow rule. It includes the effect of linear thermo-elasticity, yielding, plastic flow, isotropic strain hardening, strain rate hardening, softening due to adiabatic heating and damage. The equivalent von- Mises stress $\overline{\sigma}$ of the Johnson-Cook model is defined as;

$$\overline{\sigma}\left(\overline{\varepsilon}^{pl},\ \dot{\overline{\varepsilon}}^{pl},\hat{T}\right)=\left[A+B\left(\overline{\varepsilon}^{pl}\right)^{n}\right]\left[1+C\ln\left(\frac{\dot{\overline{\varepsilon}}^{pl}}{\dot{\varepsilon}_0}\right)\right]\left[1-\hat{T}^{m}\right] \tag{1}$$

Where A, B, n, C and m are material parameters determined from different mechanical tests. $\overline{\varepsilon}^{pl}$ is equivalent plastic strain, $\dot{\overline{\varepsilon}}^{pl}$ is equivalent plastic strain rate, $\dot{\varepsilon}_0$ is a reference strain rate and $\hat{T}$ is non-dimensional temperature defined as;

$$\hat{T}=\left(T-T_0\right)/\left(T_{melt}-T_0\right),\ T_0\le T\le T_{melt} \tag{2}$$

where T is the current temperature, T_{melt} is the melting point temperature and T_0 is the room temperature. Johnson and Cook (1985) extended the failure criterion proposed by Hancock and Mackenzie [12] by incorporating the effect of strain path, strain rate and temperature in the fracture strain expression, in addition to stress triaxiality. The fracture criterion is

based on the damage evolution wherein the damage of the material is assumed to occur when the damage parameter, ω, exceeds unity;

$$\omega = \sum \left(\frac{\Delta \bar{\varepsilon}^{\mathrm{pl}}}{\bar{\varepsilon}_f^{pl}} \right) \tag{3}$$

Where $\Delta\bar{\varepsilon}^{\mathrm{pl}}$ is an increment of the equivalent plastic strain, $\bar{\varepsilon}_f^{pl}$ is the strain at failure, and the summation is performed over all the increments throughout the analysis. The fracture model proposed by Johnson-Cook takes into account the effect of stress triaxiality, strain rate and temperature on the equivalent failure strain. The equivalent fracture strain $\bar{\varepsilon}_f^{pl}$ is expressed as;

$$\bar{\varepsilon}_f^{pl}\left(\frac{\sigma_m}{\bar{\sigma}},\ \dot{\bar{\varepsilon}}^{\mathrm{pl}},\hat{\mathrm{T}} \right) = \left[D_1 + \mathrm{D}_2 \exp\left(-\mathrm{D}_3 \frac{\sigma_m}{\bar{\sigma}} \right) \right] \left[1 + D_4 \ln\left(\frac{\dot{\bar{\varepsilon}}^{\mathrm{pl}}}{\dot{\varepsilon}_0} \right) \right] \left[1 + D_5 \hat{\mathrm{T}} \right] \tag{4}$$

Where $\mathrm{D}_1 - \mathrm{D}_5$ is material parameters determined from different mechanical tests, $\frac{\sigma_m}{\bar{\sigma}}$ is the stress triaxiality ratio and σ_{m} is the mean stress s^{-1}. The associated high strain rate and temperature further complicates the failure process in perforation problems. The strain at failure is assumed to be dependent on a non-dimensional plastic strain rate, a dimensionless pressure-deviatoric stress ratio, (between the mean stress and the equivalent von-Mises stress) and the non-dimensional temperature, defined earlier in the Johnson-Cook hardening model. When material damage occurs, the stress-strain relationship no longer accurately represents the material behavior, ABAQUS [13]. The use of stress-strain relationship beyond ultimate stress introduces a strong mesh dependency based on strain localization i.e., the energy dissipated decreases with a decrease in element size. Hillerborg's [14] fracture energy criterion has been employed in the present study to reduce mesh dependency by considering stress-displacement response after the initiation of damage. The section of the pole was assigned Fe250 steel and the ultimate tensile strength is 410 MPa, IS 2713:1980 [15], is almost equivalent to the ultimate tensile strength proposed by Iqbal et al. [16]. The material properties of the steel reinforcing bar has been shown in Table 1.

Table 1 – Material parameters for steel reinforcing bar

Description	**Notations**	**Numerical value**
Modulus of elasticity	E (N/mm^2)	203000
Poisson's ratio	V	0.33
Density	ρ (Kg/m^3)	7850
Yield Stress constant	A (N/mm^2)	304.330
Strain hardening constant	B (N/mm^2)	422.007
	n	0.345
Viscous effect	C	0.0156
Thermal softening constant	m	0.87
Reference strain rate	$\dot{\varepsilon}_0$	.0001 s^{-1}
Melting temperature	θ_{melt} (K)	1800
Transition temperature	$\theta_{\mathrm{transition}}$ (K)	293
Fraction strain constant	D_1	0.1152
	D_2	1.0116
	D_3	-1.7684
	D_4	-0.05279
	D_5	0.5262

3 Numerical Investigations

The steel pole and simple vehicle were modelled using commercial finite element package ABAQUS/CAE. The choice of pole is based through investigations which has been discussed in this Section. The properties of metallic pole available in the literature, see Table 1 proposed by Iqbal et al. [16] has also been discussed in the previous Section. The finite element modelling and mesh convergence study on pole has been conducted and discussed below.

3.1 Selection of Metallic Highway Poles

As per IS 2713:1980 [15], the metallic poles were classified as steeped pole (TP) and swaged poles (SP) and the total length of pole was varying from 7 to 16 m. The stepped and swaged poles were designated as 410 TP-xx and 410 SP-xx, whereas the "xx" designates the order of number starting from 0 to 80 and 410 is ultimate tensile strength of pole. However, in the present study, the swaged steel pole of height 11 m was considered. The reason behind choosing the particular case is the light poles for conventional highway lighting applications support luminaire mounting heights ranging from approximately 30 to 50 ft (9.1 to 15.2 m), IESNA, RP-8-05 [17]. The diameter corresponding thickness of pole at bottom, middle and top were 165.1 × 4.50 mm, 139.7 × 4.50 mm and 114.3 × 3.65 mm, respectively, see Fig. 1, are considered in the present study.

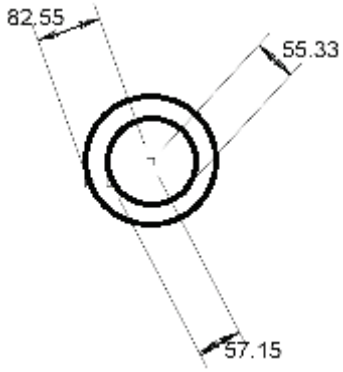

Fig. 1 – Schematic of metallic pole.

3.2 Finite Element Modelling of Steel Pole and Vehicle

The geometry of steel pole as well as simple vehicle is similar to the shape of car were developed using ABAQUS/CAE. The geometry of pole was modelled as deformable body whereas the vehicle was modelled as rigid. The length and height of vehicle (striker) model was 3.61 and 1.21 m respectively, is the conventional geometry of the car considered in the present study is shown in Fig 2(a)-(b), having moment of inertia, I_{xx}=0.105 m^4, I_{yy}=0.252 m^4 and I_{zz}=0.224m^4. The mass of vehicle was considered small car equivalent to1200 kg which is available in the market. The vehicle model (striker) in the present study were modelled as analytically rigid due to their high rigidity in comparison to the metallic poles. The vehicle was assigned initial velocities of equivalent to the speed of vehicles, i.e. 40, 80, 120 and 160 km/h. The contact between the vehicle and pole was modelled by employing the kinematic contact algorithm. The striker was considered as master and the contact surface of pole as slave surface. The friction between the target and impactor was considered insignificant, i.e. 0.05. The typical finite element modelling of steel pole has been shown in Fig. 3(a)-(d).

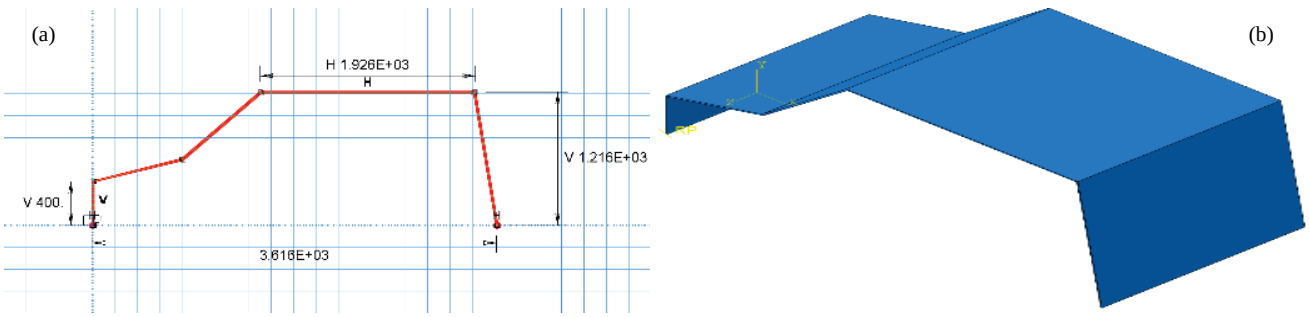

Fig. 2 – (a) Side view (mm) and (b) isometric view of typical vehicle model.

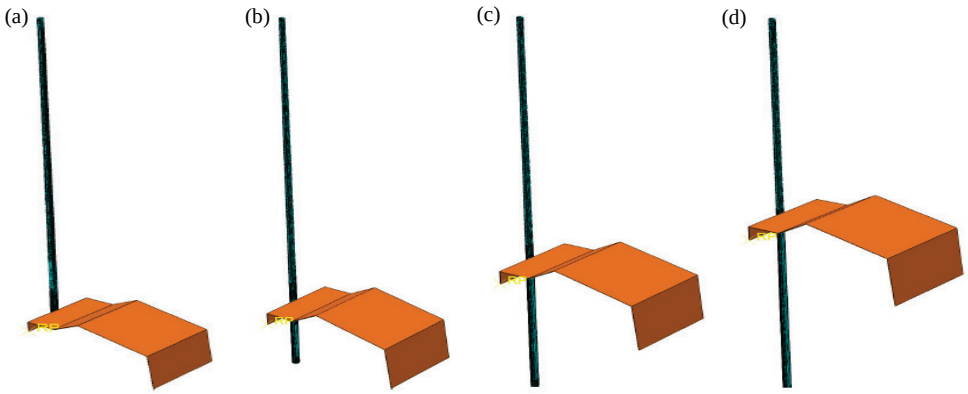

Fig. 3 – Finite element model of pole and vehicle at (a) 0 (b) 2 (c) 4 and (d) 5.5 m impact location.

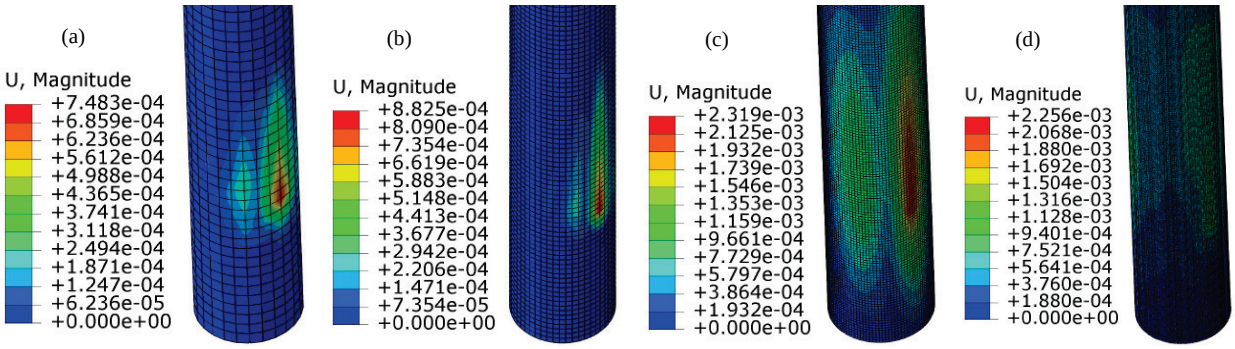

Fig. 4 – Maximum deflection on steel pole of (a) 20 (b) 10 (c) 5 and (d) 2 mm mesh sizes.

3.3 Mesh convergence study

The steel pole was meshed using structured elements of 8 noded hexahedral linear brick element. A detailed mesh sensitivity analysis has been carried out to understand the influence of mesh size. The size of element was varied as 20 × 20 × 20 mm, 10 × 10 × 10 mm, 5 × 5 × 5 mm and 2 × 2 × 2 mm. The mesh convergence study have been studied considering the mass and speed of vehicle as 1200 kg and 120 kmph respectively. The velocity and mass of vehicle was assigned through reference point and the reference point was placed on rigid body of vehicle. The total number of elements in the pole were 14326, 23886, 53762 and 612960 against 20, 10, 5 and 2 mm mesh size respectively. The bottom boundary condition of pole was assumed to be fixed with help of option "Encaster" fully built-in, i.e. U1 = U2 = U3 = UR1 = UR2 = UR3 = 0. The component U1, U2 and U3 are the translations in x, y and z directions respectively. In case of UR1, UR2 and UR3 are rotational translation in x, y and z directions respectively. The location of impact was kept arbitrarily at bottom of the pole, i.e. 150 mm from fixed base. The predicted results were compared in terms of maximum deflection and Mises stresses in steel, see Fig. 4(a)-(d) and 5(a)-(d), respectively. It is observed that the maximum deflection in pole was found to be 0.74, 0.88, 2.3 and 2.25 mm against 20, 10, 5 and 2 mm mesh size respectively. The Mises stresses corresponding to maximum deflection in pole were found to be 224, 270, 292 and 498 MPa against 20, 10, 5 and 2 mm mesh size respectively. The maximum deflection of pole was found to be 2.3 mm against 5 mm mesh size however the strength of material was found to be increased with decrease of mesh size. The mesh size of pole 2 × 2 × 2 mm, in light of achieving the ultimate tensile strength of pole is 410 MPa as per [15]. Therefore, it is concluded that the mesh size of 2 mm was found suitable for further analysis. The size of element was therefore considered to be 2 mm^3 and the aspect ratio unity in all the simulations. Away from the impact region, however, the size of element was slightly increased keeping the aspect ratio unity. The analysis was divided into 40 frames within a time frame of 0.005 second. A CPU time for impact simulation event took around 1.36, 6.30, 12.1o and 18.45 hours by 20, 10, 5 and 2 mm mesh size respectively. The present study incorporates plastic-elastic-thermo shocks considering high velocity compact during vehicle collision. As the strain-rate increases, the effect from vehicle-pole

collision impact becomes a shock wave phenomenon and the effect of strain rate is incorporated in JC strength and damage model $\left[1+\mathrm{C}\ln\left(\frac{\dot{\bar{\varepsilon}}^{pl}}{\dot{\varepsilon}_0}\right)\right]$ and $\left[1+\mathrm{D}_4\ln\left(\frac{\dot{\bar{\varepsilon}}^{pl}}{\dot{\varepsilon}_0}\right)\right]$ respectively, please see Equations 1 and 4.

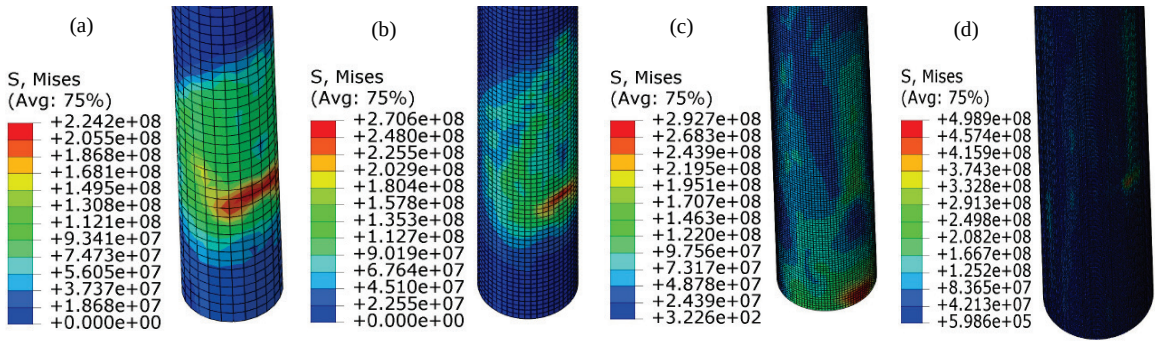

Fig. 5 – Maximum von-Mises stresses on pole of (a) 20 (b) 10 (c) 5 and (d) 2 mm mesh sizes.

4 Results and Discussion

Three-dimensional finite element analysis has been carried out in order to study the response of highway steel pole against vehicle impact using ABAQUS/CAE. The simulations were carried out against vehicle impact subjected to varying speed and mass of vehicle, varying thickness and impact location of pole. The response of elements were observed in terms of von-Mises stresses, deflection and reaction forces of highway pole therein were presented and discussed in this Section.

4.1 Influence of varying speed of vehicle

The simulations were carried out on metallic pole to study the influence of varying speed of vehicle. The speed of vehicle was varied as 40, 80, 120 and 160 kmph and the mass of vehicle was kept constant, 1200 kg, see Fig. 6. The unit of the von-Mises stress in the contour is "N/m^2". The maximum von-Mises stresses at the pole were found to be 433, 498, 498 and 527 MPa for 40, 80, 120 and 160 kmph respectively. The stress developed in the pole was found to be higher at particular location, i.e. local effect and it may be due to the change in rotation vehicle. The maximum stress in steel pole was about 498 and 527 Mpa against the speed of vehicle at 120 and 160 kmph respectively and it is found to be more vulnerable. For the convenience of reader, the image of deformation was shown with free edge of mesh was shown in Fig. 6(a-ii)-(d-ii). The stress on pole was found to be same against 120 and 80 kmph and however, there is only local failure noticed at 80 kmph whereas the global failure was noticed against 120 kmph speed. It is observed that the pole failed against 80 kmph and it is clearly seen from Fig. 6(b-i)-(b-ii), whereas the pole was found to be un-deformed at 40 kmph, see Fig. 6(a-i)-(a-ii). To understand the stress variation through the entire impact event of 0.005 second, the von-Mises stresses on pole near to the base at node 13980 at varying speed of vehicle was measured and shown in Fig. 7. It is concluded that the steel pole was found to be able to withstand a vehicle impact load with speed 80 kmph without any significant damage. So, when impact speed greater than 80 kmph encountered in the steel pole, special care should be taken for the impact to minimise chances of failure.

The displacement of pole against impact load of varying speed of vehicle is shown in Fig. 8(a)-(d). The unit of the displacement contours was shown in "meter". The maximum deflection was found to be 0.61, 3.53, 2.10 and 2.25 mm against 40, 80, 120 and 160 kmph speed respectively. It is observed that the deflection developed in the pole was found to be insignificant when the impact speed of 40 kmph, whereas the maximum displacement was found to be against 80 kmph speed. At 120 and 160 kmph speed, the displacement in pole was found reduced almost by 40% as compared to the speed of 80 kmph. The reason may be due to the fact that the less contact time causes the vehicle to bounce back when the speed of vehicle is beyond 80 kmph speed.

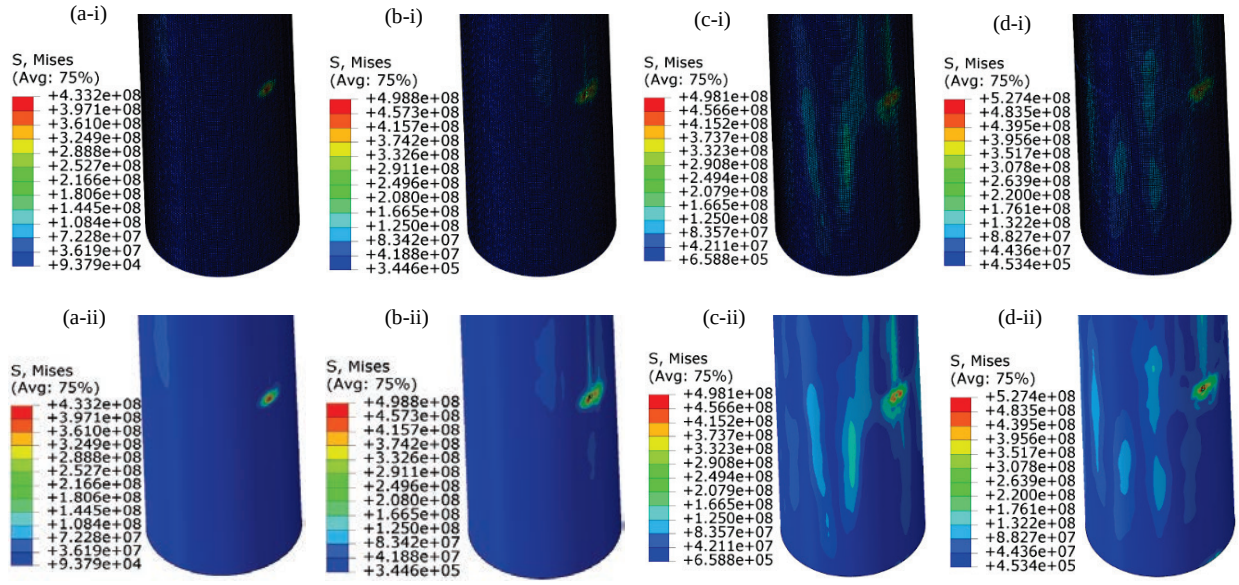

Fig. 6 – von-Mises stresses in pole with (i) mesh and (ii) free edge by (a) 40 (b) 80 (c) 120 and (d) 160kmph speed at 5ms.

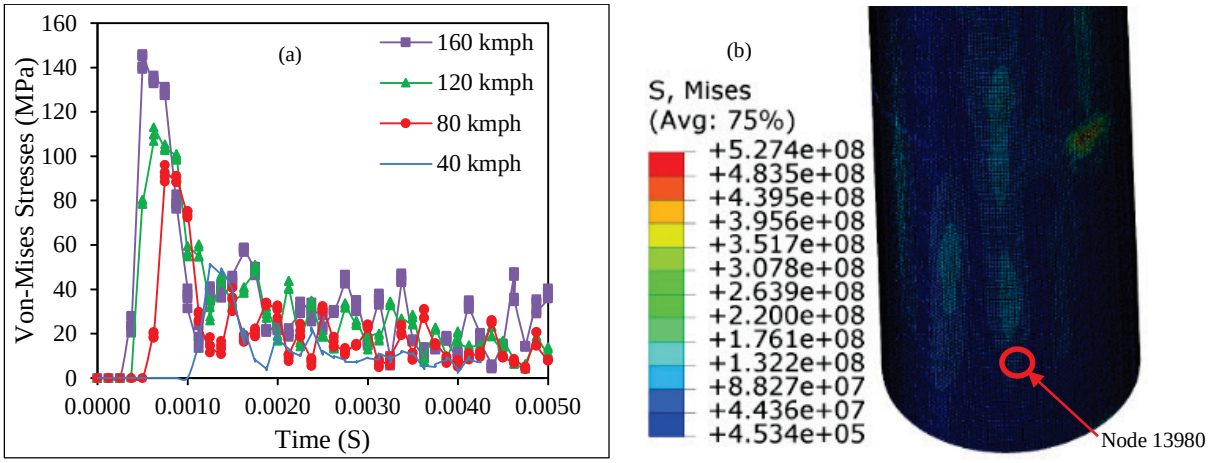

Fig. 7 –Von-Mises (a) stresses on pole near to the base at varying speed of vehicle at node (b) 13980 of typical case.

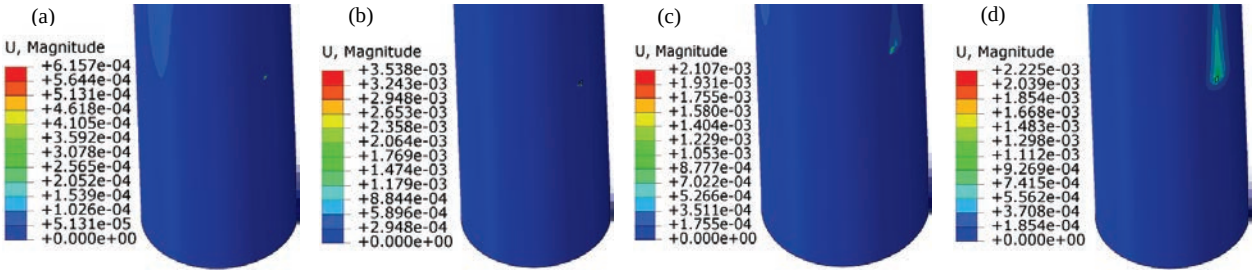

Fig. 8 – Deflection (m) of pole against (a) 40 (b) 80 (c) 120 and (d) 160 kmph speed at 5 ms.

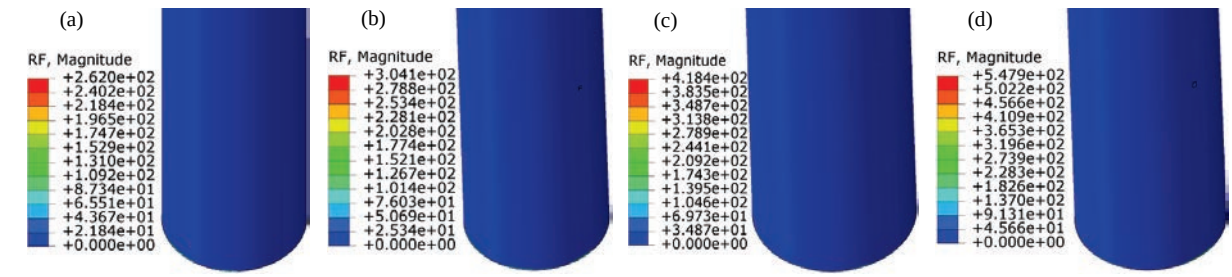

Fig. 9 – Reaction forces (kg) by pole against (a) 40 (b) 80 (c) 120 and (d) 160 kmph speed at 1.5 ms.

The maximum reaction forces of the pole has been obtained numerically at a specific speed of vehicle is compared, see Fig. 9. The resistance offered by the pole was found to be 262, 304, 418 and 548 kg against 40, 80, 120 and 160 kmph speed respectively. It is observed that the reaction forces offered by the pole were increased almost linearly as increase of speed of vehicle. Therefore, it is concluded that the performance and behavior of pole during impact depends on the speed of the vehicle and higher speed leads to larger damage to the systems.

4.2 Influence of varying mass of vehicle

The simulations were carried out on steel pole to study the influence of varying mass of vehicle. The mass of vehicle was varied as 600, 1200, 1800 and 2400 kg and the velocity of vehicle was kept constant, 120 kmph. The maximum von-Mises stresses at the pole were found to be 532, 498, 511 and 473 MPa for 600, 1200, 1800 and 2400 kg mass respectively. The stress developed in the pole was found to be higher at impact location, i.e. local effect. The maximum stress in steel pole was about 532 Mpa against the mass of vehicle 600 kg and it is found to be more vulnerable. The stress induced on pole was 473 MPa due to the mass of 2400 kg and it is noticed only excessive stresses, see Fig. 10(a)-(c). However, at 600, 1200 and 1800 kg mass, there is a clear punching and hole in elliptical shape was observed, see Fig. 10(a)-(c). It was also observed that the pole failed against the mass of upto 1800 kg, whereas the pole was found to be safe against the mass of vehicle 2400 kg, see Fig. 10(d). To confirm the accuracy of simulations since there is a contradictory results, the stress function of time corresponding varying mass of vehicle is shown in Fig. 11. The stress was measured from two locations, i.e. near to the base at node 13980 and near to the impact zone at node 69223. It was observed that the stresses against varying mass of vehicle is found to be almost same. It is concluded that the system was found to fail by ductile hole and enlargement if the stresses exceeds 490 MPa in case of lower or higher mass of the vehicle.

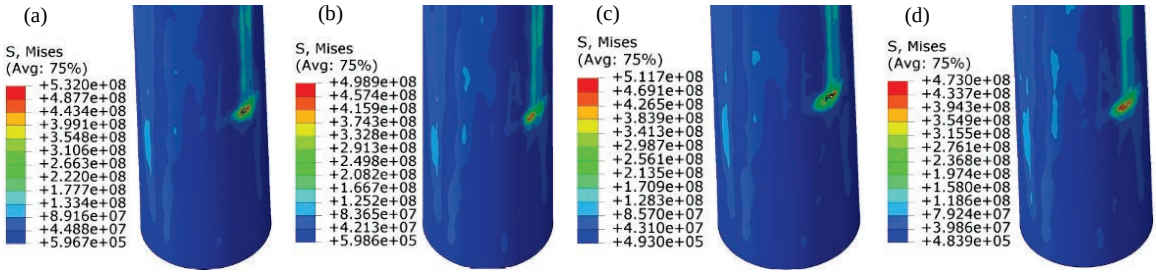

Fig. 10 – von-Mises stresses in pole by (a) 600 (b) 1200 (c) 1800 and (d) 2400 kg speed at 5 ms.

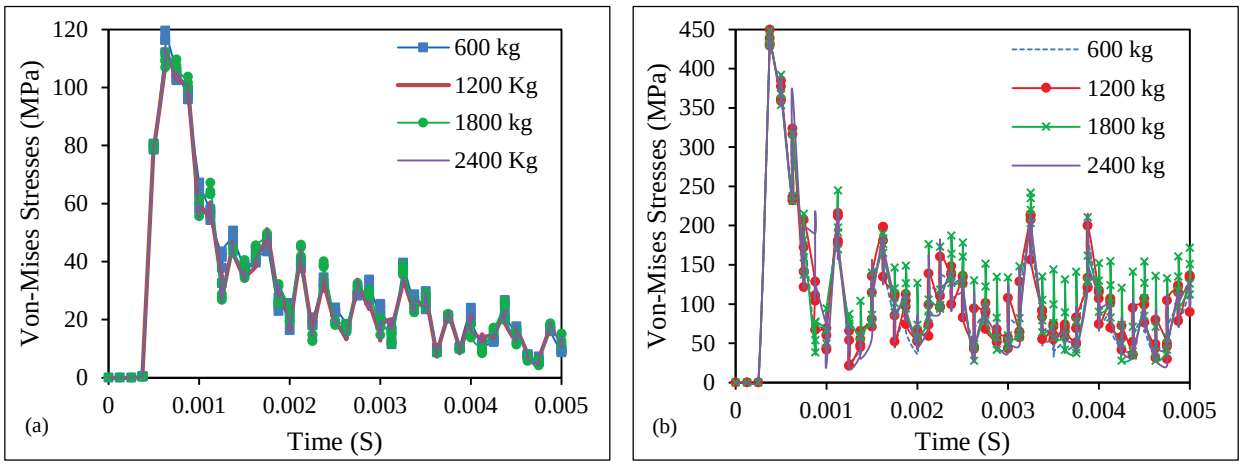

Fig. 11 – Von-Mises stresses on pole (a) near to the base at node 13980 and (b) near to the impact zone at node 69223 against varying mass of vehicle.

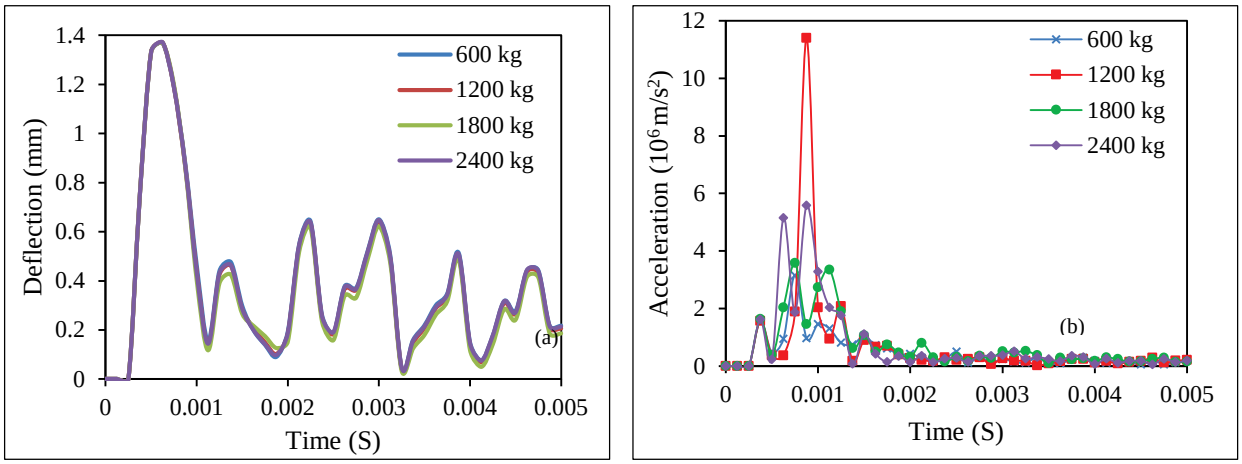

Fig. 12 – Response of pole near to the impact zone at node 69223 in terms of (a) deflection and (b) acceleration.

Further to confirm the accuracy of simulations, the deflections and acceleration function of time corresponding to varying mass of vehicle was measured and shown in Fig. 12. The deflections and acceleration were measured from the locations, i.e. near to the impact zone at node 69223. It is observed that the deflections against varying mass of vehicle is found to be same resulting the effect of mass of vehicle is insignificant. The maximum acceleration 3.1, 11.3, 3.5 and 5.5 × 10^6 m/s^2 was observed due to impact of mass 600, 1200, 1800 and 2400 kg mass respectively. Overall, it is observed that the acceleration of target was affected significantly and doesn't have continuity due to varying mass of vehicle. The accelerations of target was found to be increased from 3.1 to 11.3 Mega m/s^2 when the mass of vehicle varied from 600 to 1200 kg. It may be due to only the mass of vehicle and cause increase in acceleration in the pole. Whereas, the acceleration of target was found to be decreased significantly when the mass of vehicle increased from 1200 to 1800 kg. It may be due to the overturning and rebounding of the vehicle due to higher mass. In addition to that, there may be a lack of friction coefficient which has been assigned in the simulations and the impactor was modelled as rigid body. The rigid body motion during impact and shock may affect the overall result. Similarly, the acceleration of target was found to be increased from 3.5 to 5.5 Mega m/s^2 when the mass of vehicle increased from 1800 to 2400 kg. It may be due to the increase in actual mass of vehicle, however, the increment in the acceleration is insignificant. Hence it is concluded that the mass of vehicle of 1200 kg is found to be critical and pole is to be designed accordingly.

The displacement of pole against impact load of varying speed of vehicle is shown in Fig. 13(a)-(d). The maximum deflection was found to be 1.77, 2.10, 3.35 and 1.66 mm against 600, 1200, 1800 and 2400 kg mass respectively. At 1800 kg mass, the displacement in pole was found to be highest among the chosen case. It is observed that the deflection developed in the pole was found to be increased when the impact speed mass increases upto 1800 kg almost linearly, however the maximum displacement by 2400 kg mass was found to be decreased almost 50% as compared to 1800 kg mass.

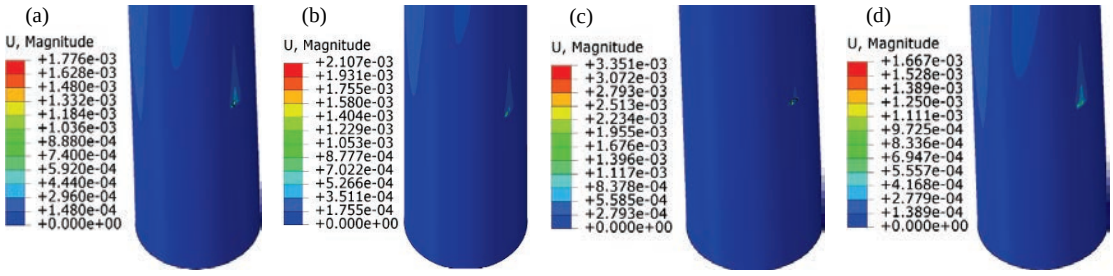

Fig. 13 – Deflection (m) of pole against (a) 600 (b) 1200 (c) 1800 and (d) 2400 kg mass at 5 ms.

The maximum reaction forces of the pole has been obtained numerically at a specified mass of vehicle at 1.5 and 5 millisecond is compared, see Fig. 14. At 1.5 millisecond, the resistance offered by the pole was found to be 409, 418, 394 and 421 kg against 600, 1200, 1800 and 2400 kg mass respectively. At 5 millisecond, the resistance offered by the pole was found to be 154, 141, 131 and 146 kg against 600, 1200, 1800 and 2400 kg mass respectively. It is observed that the reaction forces offered by the pole was almost consistent, irrespective of mass of vehicle. Therefore, it is concluded that the performance and behavior of pole during impact is not depended on the mass of vehicle upto the range of 2400 kg.

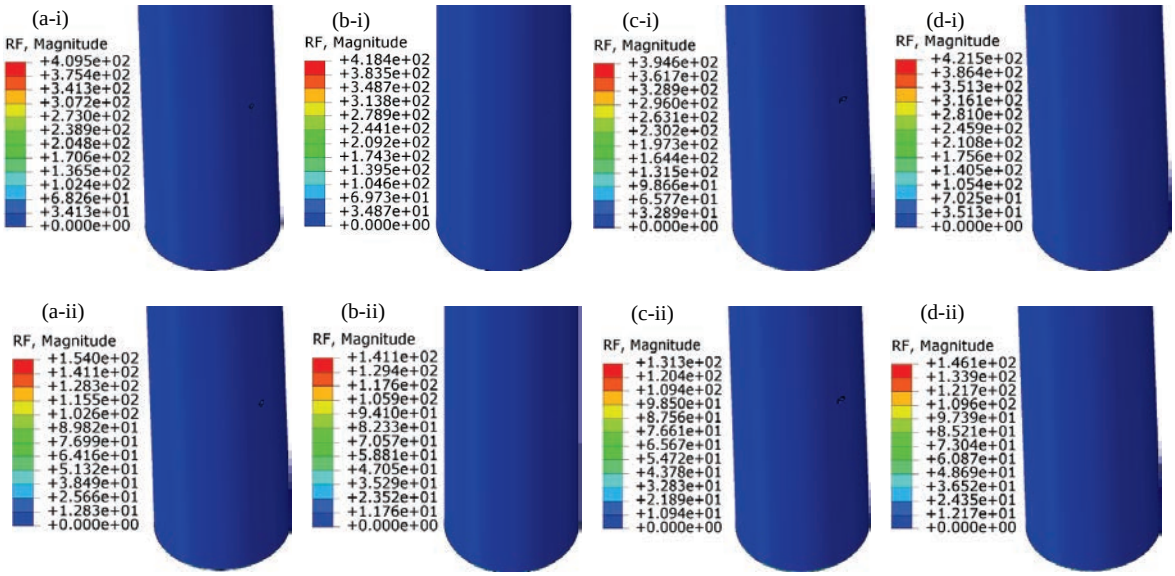

Fig. 14 – Forces (kg) against (a) 600 (b) 1200 (c) 1800 and (d) 2400 kg mass at (i) 1.5 and (ii) 5 ms.

4.3 Influence of varying thickness of cylindrical pole

The simulations were carried out on steel pole to study the influence of varying thickness of cylindrical pole (25%, 50% and 75% reduction as compared to initial thickness) considering the fact that thickness of pole may be reduced due to excessive corrosion. The thickness of shells on pole was varied as 4.5, 3.375, 2.25 and 1.125 mm and the speed and mass of vehicle was kept constant, 120 kmph and 1200 kg respectively. The maximum von-Mises stresses at the pole were found to be 498, 358, 530 and 567 MPa for 4.5, 3.375, 2.25 and 1.125 mm thickness respectively, see Fig. 15(a)-(d). The maximum stress in steel pole with thickness of 1.125 mm was about 567 Mpa and it is found to be more vulnerable. The stress on pole 358 MPa is lowest one, there is only excessive stresses noticed without punching and damage, see Fig. 15(b). However, at 2.25 and 1.125 mm thickness, there is clear punching and hole in elliptical shape, see Fig. 15(c)-(d). In addition to that, the area of damage in 1.125 mm thick pole was found to be increased significantly as compared to the pole with 2.25 mm.

Further to confirm the accuracy of simulations, the stresses versus time corresponding to varying thickness of pole is obtained and shown in Fig. 16. The stress was measured from the locations, near to the base at node 13980. It was observed that the stresses on pole as well as area under the stress-time curve was found increased with decrease in thickness of pole. The stress at 1.125 mm thick pole was found to be reduced slightly however the area under this curve is large. The reason may be due to lesser thickness and cause bucking and global deformation of shell leads to absorb more energy. It is concluded that the system with more than 50% reduction of thickness is found to fail significantly and proper maintenance should be taken care to avoid excessive corrosion.

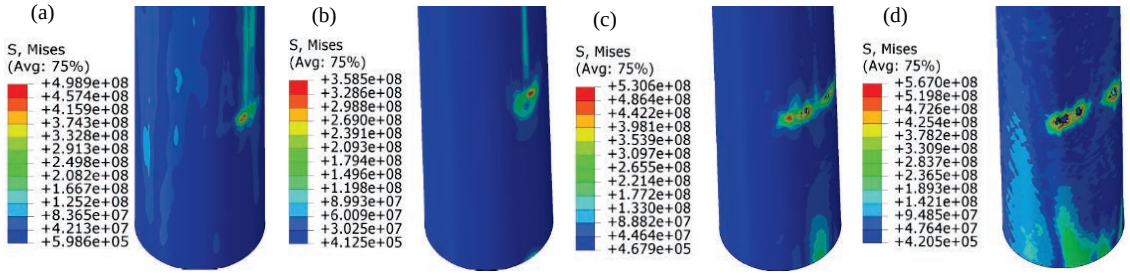

Fig. 15 – von-Mises stresses in pole with (a) 4.5 (b) 3.375 (c) 2.25 and (d) 1.125 mm thickness at 5 ms.

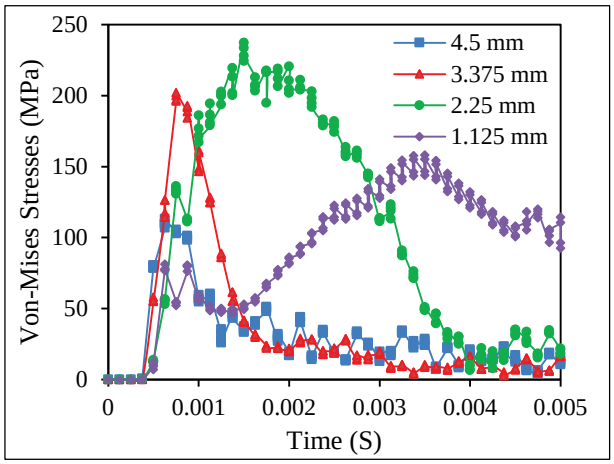

Fig. 16 – Von-Mises stresses on pole near to the base at varying thickness at node 13980.

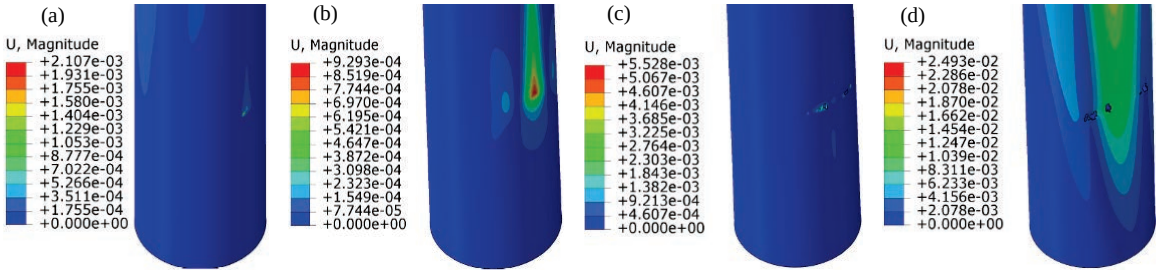

Fig. 17 – Deflection (m) of pole having (a) 4.5 (b) 3.375 (c) 2.25 and (d) 1.125 mm thickness 5 ms.

The displacement of pole with varying thickness is shown in Fig. 17(a)-(d). The maximum deflection of pole with 4.5, 3.375, 2.25 and 1.125 mm thickness was found to be 2.10, 0.92, 5.52 and 24.93 mm respectively. At 1.125 mm thickness, the displacement in pole was found to be highest among the chosen configurations. It is observed that the deflection developed in the pole was found to be increased with decrease in thickness of pole however, the pole with 3.375 mm thickness was found to be decreased significantly. Therefore, it is concluded that the response of pole performs better if the thickness of pole reduces upto 25% from the initial thickness of pole and the 3.375 mm thickness may be considered as optimum design thickness.

The reaction forces offered by the pole has been obtained numerically at a specified mass and speed of vehicle at 1.5 millisecond, see Fig. 18. The forces offered by the pole with 4.5, 3.375, 2.25 and 1.125 mm thickness was found to be 418, 211, 1067 and 678 kg respectively. It is observed that the forces offered by the pole with varying thickness of pole were inconsistent. The reaction forces on pole with 3.375 mm thickness were found lowest whereas the pole with 2.25 mm were found highest. The reaction force increases to the system leads to more damage and is more vulnerable, see Fig. 18(c)-(d). The conclusions in light of reaction forces were similar to deflection characteristics, the response of pole is found better if the thickness of pole reduces upto 25% from the initial thickness of pole and the 3.375 mm thickness may be considered as optimum design thickness.

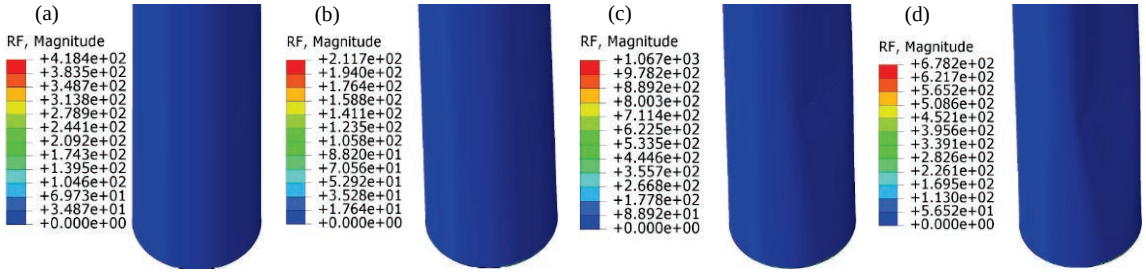

Fig. 18 – Forces (kg) by pole with (a) 4.5 (b) 3.375 (c) 2.25 and (d) 1.125 mm thickness at 1.5 ms.

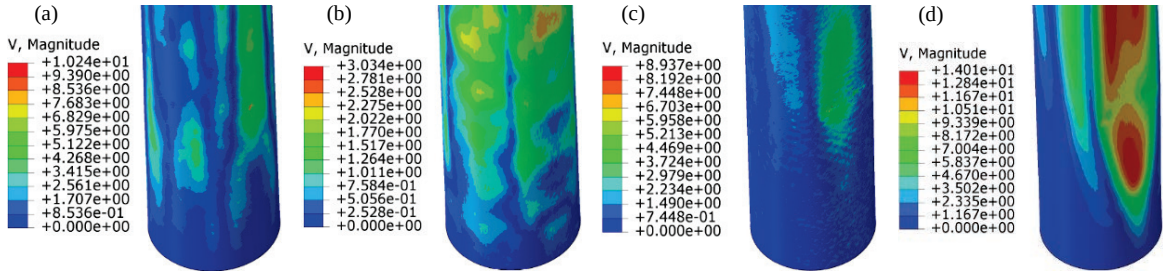

Fig. 19 – Velocity (m/s) in pole with (a) 4.5 (b) 3.375 (c) 2.25 and (d) 1.125 mm thickness at 1.5 ms.

The velocity transferred to the pole has been obtained numerically at a specified mass and speed of vehicle at 1.5 millisecond is compared, see Fig. 19. The velocity transferred to the pole with 4.5, 3.375, 2.25 and 1.125 mm thickness was found to be 10.2, 3.03, 8.9 and 14.0 m/s respectively. It is also observed that the velocity transferred by the pole was inconsistent with varying thickness of pole. The velocity on pole with 3.375 mm thickness was found least whereas the pole with 1.125 mm was found highest. The velocity distribution increases to the system leads to more damage and is more vulnerable, see Fig. 19(d). The conclusions were similar to deflection and reaction characteristics, the performance of pole is found to be better if the thickness of pole reduces only upto 25% from the initial thickness of pole.

4.4 Influence of varying impact location on pole

The simulations were carried out on steel pole to study the influence of varying impact locations along the height of pole considering the fact that impact location may vary due to accident and flying object of large masses. The impact location in pole was varied as 0.15, 2, 4 and 5.5 m from base and the speed and mass of vehicle was kept constant, 120 kmph and 1200 kg. The maximum von-Mises stress in pole were found to be 498, 507, 509 and 512 MPa for 0.15, 2, 4 and 5.5 m from base respectively, see Fig. 20(a)-(d). The maximum stress in steel pole against 5.5 m impact location was 512 Mpa and it is found to be more vulnerable. The stress peak was found single when 0 and 2 m impact location, whereas 4 and 5.5 m impact location causes two and three peaks of stress.

Further to confirm the accuracy of simulations, the stress versus time corresponding to varying impact lcoations is obtained and shown in Fig. 21. The stress was measured from the locations, near to the base at node 13980. The maximum stress was found to be 113, 44, 34 and 32 MPa against 0.15, 2, 4 and 5.5 m from base respectively. It was observed that the stresses on pole were found highest for 0.15 m which is close to the node 13980. The stress was shown in Fig. 20 is almost same (498-512 MPa) whereas the trend shown in Fig. 21 is decreasing significantly (113-32 MPa). The reason for highest stress i.e. 113 MPa is due to the location of node 13980 is close to 0.15 m, whereas in case of stresses (44, 34 and 32) the other impact location located far away from 13980. It is concluded that the performance of pole may not be affected if the incidence took place within 50% height of pole from base.

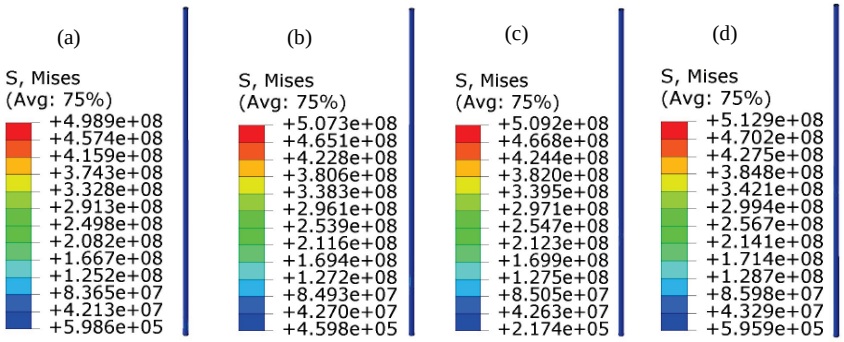

Fig. 20 – von-Mises stresses in pole by impact at (a) 0 (b) 2 (c) 4 and (d) 5.5 m from base at 5 ms.

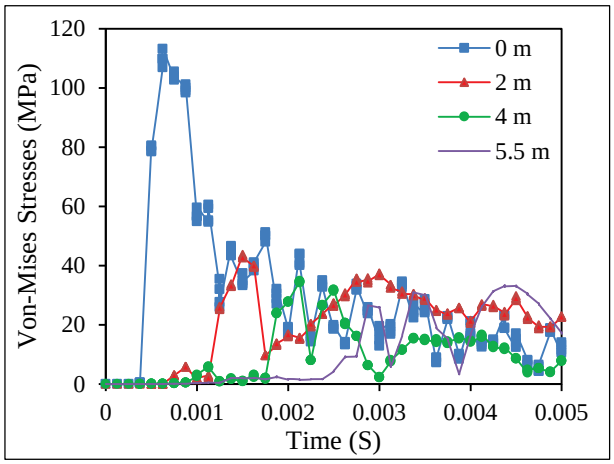

Fig. 21 – Von-Mises stresses on pole near to the base at varying impact location at node 13980.

The displacement of pole against varying the impact location is shown in Fig. 22(a)-(d). The maximum deflection of pole was 2.10, 3.67, 2.82 and 2.80 mm against impact and location of 0.15, 2, 4 and 5.5 m from base respectively. The displacement in pole was found to increase from 2.1 to 3.67 mm when the impact location increased from 0.15 to 2 m. The deflection due to impact at 4 and 5.5 m was found to be almost same, see Fig. 22(c)-(d). It is observed the maximum deflection when the impact takes place one fifth of height of pole whereas the deflection was almost same when the impact at one third and half of height. The deflection at one fifth of height of pole was found to be increased by 30% compared to the impact at one third height of pole. The deflection at one fifth of height of pole was found to be increased by 75% compared to the impact at one hundred height of pole. Therefore, it is concluded that the place nearest to one fifth height of pole may be taken care while designing the pole.

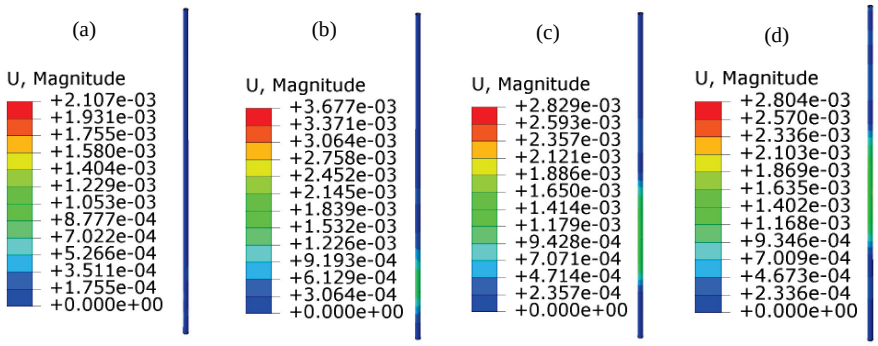

Fig. 22 – Deflection (m) in pole by impact at distance (a) 0 (b) 2 (c) 4 and (d) 5.5 m from base at 5 ms.

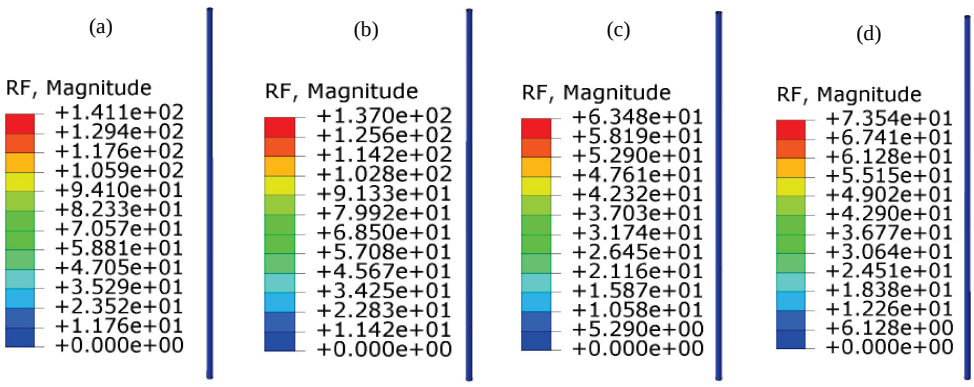

Fig. 23 – Forces (kg) in pole by impact at distance (a) 0 (b) 2 (c) 4 and (d) 5.5 m from base at 5 ms.

The reaction forces of the pole has been obtained numerically at a specified mass and speed of vehicle at 5 millisecond, see Fig. 23. The reaction forces offered by the pole was found to be 141, 137, 63 and 73 against impact location of 0.15, 2, 4 and 5.5 m from base respectively. It is observed that the reaction forces offered by the pole was decreased with increasing impact distance from base. The reaction forces due to impact at one fifth and one hundredth height of pole was found to be almost same. Similarly, the reaction forces due to impact at half of height of pole was found to be increased by 15% compared to the impact at one third height of pole. Therefore, it is concluded that the place nearest to one fifth height of pole may be taken care while designing the pole.

5 Conclusion

The present study addresses the finite element investigation of the behavior of steel pole subjected to vehicle impact loading. Numerical simulations were carried out using ABAQUS/Explicit finite element model to predict the response of steel pole against varying impact speed, mass, location of impact and thickness of cylindrical pole. The response of pole was studied in terms of von-Mises stresses, deflection and reaction forces, and the following conclusions were drawn.

The simulations were carried out to study the influence of varying speed of vehicle and the speed of vehicle was 40, 80, 120 and 160 kmph. It is concluded that the steel pole was found to be able to withstand a vehicle impact load with speed 80 kmph without any significant damage. So, when impact speed greater than 80 kmph is encountered in the steel pole, special care should be taken for the impact to minimize chances of failure. In light of reaction forces, it is concluded that the performance of pole during impact is depends on the speed of vehicle and higher speed leads to larger in damage to the systems.

The simulations were carried out to study the influence of varying mass of vehicle and the mass of vehicle was 600, 1200, 1800 and 2400 kg. It is concluded that the systems was experiencing ductile hole and enlargement if the stresses exceeds 490 MPa either of lower or higher the mass of vehicle. It is observed that the deflection developed in the pole was found to be increased when the impact speed mass increases upto 1800 kg almost linearly, however the maximum displacement by 2400 kg mass was found to be decreased almost 50% as compared to 1800 kg mass. It is concluded that the reaction forces by pole during impact is not affecting by the mass of vehicle upto the range of 2400 kg.

The simulations were carried out to study the influence of varying thickness of cylindrical pole (25%, 50% and 75% reduction as compared to initial thickness) considering the fact that thickness of pole may be reduced due to excessive corrosion. It is concluded that the system was found to fail significantly when the thickness reduces more than 50%. It is concluded in light of deflection and reaction characteristics, the performance of pole was found to be better if the thickness of pole reduces upto 25% from the initial thickness of pole.

The simulations were carried out to study the influence of varying impact locations along the height of pole considering the fact that impact location may vary due to accident and flying object of large masses. It is concluded that the performance of pole may not be affected if the impact event took place within 50% height of pole from base. It is also concluded in light of deflection and reaction forces, the place nearest to one fifth height of pole was found vulnerable and proper care may be taken.

REFERENCES

[1]- A. Elmarakbi, K. Sennah, M. Samaan, P. Siriya, Crashworthiness of motor vehicle and traffic light pole in frontal collisions. J. Transp. Eng-ASCE, 132(9) (2006)722-733. doi:10.1061/(ASCE)0733-947X(2006)132:9(722)

[2]- T. Le, A. Abolmaali, S.A. Motahari, W. Yeih, R. Fernandez, Finite element-based analyses of natural frequencies of long tapered hollow steel poles. J. Constr. Steel Res. 64(3) (2008) 275–284. doi:10.1016/j.jcsr.2007.08.006

[3]- J. Jung, A. Abolmaali, Y. Choi, Finite-element analysis of tapered steel and fiber-reinforced plastic bridge camera poles. J. Bridge Eng. 11(5) (2006) 611–617. doi:10.1061/(ASCE)1084-0702(2006)11:5(611)

[4]- B. Vivek , S. Sharma, P. Raychowdhury, S. Ray-Chaudhri, A study on failure mechanism of self-supported electric poles through full-scale field testing. Eng. Fail. Anal. 77 (2017) 102–117. doi:10.1016/j.engfailanal.2016.12.019

[5]- Q. Lu, H.R. Karimi, K.G. Robbersmyr, A data-based approach for modeling and analysis of vehicle collision by lPV-ARMAX models. J. Appl. Math. 2013 (2013) 1-9. doi:10.1155/2013/452391

[6]- H. Sharma, S. Hurlebaus, P. Gardoni, Performance-based response evaluation of reinforced concrete columns subject to vehicle impact. Int. J. Impact Eng. 43(2012) 52-62. doi:10.1016/j.ijimpeng.2011.11.007

[7]- F. Chen, C. Tang, J. Zhang, A study on the impact between car to circular concrete pole. In: Proceedings of Eighth International Conference on Measuring Technology and Mechatronics Automation, ICMTMA, Macau, China, 11-12 March, 2016. doi:10.1109/ICMTMA.2016.20

[8]- L.C. Pagnini, G. Solari, Damping measurements of steel poles and tubular towers. J. Struct. Eng. 23(9) (2001) 1085–95. doi:10.1016/S0141-0296(01)00011-6

[9]- D. Polyzois, I.G. Raftoyiannis, S. Ibrahim, Finite elements method for the dynamic analysis of tapered composite poles. Compos. Struct. 43(1) (1998) 25–34. doi:10.1016/S0263-8223(98)00088-9

[10]- G. Fu, S.J. Boulos, Finite element analysis of irregular thick plates for signal pole design. Comput. Struct. 58(1) (1996) 221–232. doi:10.1016/0045-7949(95)00134-3

[11]- G.R. Johnson, W.H. Cook, Fracture characteristics of three metals subjected to various strains, strain rates, temperatures, and pressures. Eng. Fract. Mech. 21(1) (1985) 31–48. doi:10.1016/0013-7944(85)90052-9

[12]- J.W. Hancock, A.C. Mackenzie, On the mechanisms of ductile failure in high-strength steels subjected to multi-axial stress-states. J. Mech. Phys. Solids. 24 (1976) 147–169. doi:10.1016/0022-5096(76)90024-7

[13]- ABAQUS®, V., 2014. 6.14 Documentation. Dassault Systemes Simulia Corporation.

[14]- A. Hillerborg, M. Modéer, P.-E. Petersson, Analysis of crack formation and crack growth in concrete by means of fracture mechanics and finite elements. Cement Concrete Res. 6(6) (1976) 773–781. doi:/10.1016/0008-8846(76)90007-7

[15]- IS 2713:1980, (Parts 1 to 3), Specification for tubular steel poles for overhead power lines, Bureau of Indian Standard, New Delhi, 1980

[16]- M.A. Iqbal, K. Senthil, P. Bhargava, N.K. Gupta, The characterization and ballistic evaluation of mild steel. Int. J. Impact Eng. 78 (2015) 98-113. doi:10.1016/j.ijimpeng.2014.12.006

[17]- IESNA (RP-8-05), The Illuminating Engineering Society (IES) of North America, Recommended Practice 8, Roadway Lighting, Reaffirmed in 2005.